Journal of Geophysical Research Biogeosciences

Supporting Information for

Understanding the seasonality, trends and controlling factors of Indian Ocean acidification over distinctive bio-provinces

Kunal Madkaiker[1,2,3], Vinu Valsala[3], M. G. Sreeush[5,6], Anju Mallissery[3], Kunal Chakraborty[4], Aditi Deshpande[2]

[1]Indian Institute of Technology, Delhi, New Delhi, India.
[2]Department of Atmospheric and Space Sciences, Savitribai Phule Pune University, Pune, India
[3]Indian Institute of Tropical Meteorology, Ministry of Earth Sciences, Pune, India
[4]Indian National Centre for Ocean Information Services (INCOIS), Ministry of Earth Sciences, Hyderabad, India
[5]Centre for Climate Physics, Institute for Basic Science (IBS), Busan, Republic of Korea, 46241.
[6]Pusan National University, Busan, Republic of Korea, 46241.

Contents of this file

Additional Supporting Information (Files uploaded separately)

Text S1.

Description of Study area

Region 1: WAS (Western Arabian Sea)

WAS lies around (5°-25°N and 50°-65°E) with the domination of seasonal upwelling. This region is rich in nutrients during the southwest monsoon due to coastal upwelling circulation at the Somalia and Oman coast. This supplies nutrient-rich deep water at the surface. During spring inter-monsoon, productivity reduces, and the waters become low in nutrients as the Somali Jet weakens. This region is characterized by downwelling with an intermediate level of productivity during the Northeast monsoon. WAS is a climatologically more acidic region compared to other regions, especially during the Southwest monsoon season of the tropical Indian Ocean (IO) (Takahashi et al., 2014). River discharge in this region is low, as seen in the Indus River (1681 μmol kg^{-1}) is a meager 10% of the Ganges and Brahmaputra rivers (Carter et al., 2014).

Region 2: NBoB-AI (North Bay of Bengal and Around India)

NBoB-AI is a region covering peninsular India from the eastern Arabian Sea to the western Bay of Bengal. (Sarma et al., 2015) air-sea CO_2 exchange promotes acidification along with southwest coastal BoB, while anthropogenic sources in northwest coastal BoB, have triggered aerosol acidification, transforming it into a source of CO_2 from a traditional sink. The region covering the west coast experiences upwelling during May-June. The Coastal Kelvin wave may cause some upwelling around the coast of India. The Bay of Bengal, the largest bay, forms the north-eastern part of the IO. (Carter et al., 2014) explains that BoB has two major high-alkaline river systems emptying into it, the Ganges (1966 μmol kg^{-1}) and the Brahmaputra (1114 μmol kg^{-1}) (Cai et al., 2008), with one of the most subsequent discharge points (42,000 m^3/sec), globally (Land et al., 2015), raises the surface alkalinity comparative to salinity distribution in the region (Sabine et al., 2002, 2004). This region is thus well stratified as compared to the WAS (S. S. C, Shenoi et al., 2004; S. S. C. Shenoi et al., 2002). Both above regions have warm SST but are characteristically different due to increased evaporation in the former, while riverine discharge off the latter. The physical characteristics manipulate the solubility pump natures of these two basins and cause differences in control of SST.

Region 3: EBoB-CIO (East Bay of Bengal and Central IO)

EBoB-CIO is a region extending from the Bay of Bengal to the central north equatorial IO region (see Figure S1). This region also includes the WEIO which lies around 50°E–70°E, 10°S–10°N. (Sompongchaiyakul et al., 2008) shows that the Andaman Sea (eastern BoB) has lower surface alkalinity compared to northern or western BoB. The Bay of Bengal part of this region has lower salinity, as low as 30 ppt or below, as compared to other regions due to precipitation from southwest monsoon and river discharges.

Region-4 and 5: EEIO, SEIO (Eastern and Southern Equatorial IO)

The Equatorial IO is characterized by warm SST as this region lies in the Equatorial belt along the Tropical Convergence Zone (TCZ). Unlike the Pacific and Atlantic, the eastern IO SST is warmer because of the dominant westerly component in the equatorial wind which causes deepening of thermocline in the east-west direction and downwelling along the equatorial belt (Trenary & Han, 2008; Xie et al., 2002).

Region: 6 to 8 (Southern IO and Subtropical Oligotrophic Gyre i.e. STIO, SSIO and SOG)

The subtropical or southern IO is a region of wind-driven gyre circulation. The southern IO is characterized by a subtropical anticyclonic gyre, located 30°S south of the equator. In the subtropical gyre, Ekman transport causes intensive downwelling at the center, which results in the deepening of thermoclines, pycnocline and nutriclines. Due to the deepening of nutriclines, this gyre is an oligotrophic region i.e., the biological productivity in the region is relatively low. Interdependence of surface alkalinity and salinity is observed in nearly all tropical and subtropical oceans (Millero et al., 1998), as observed in this region. In the rest of this study, we will focus on the acidification parameters in the regions identified above.

Text S2.

The seasonal mean of pH

As seen in Figure S4, pH averaged over the IO domain ranges from 8.0 to 8.13 units. During January-February-March (JFM) entire IO region appears to be of a monotonic pattern of pH, with averaged pH over the IO ranging from 8.05 to 8.09 units. Downwelling in the WAS during northeast monsoon causes a decrease in DIC, thus making the water alkaline (Fassbender et al., 2011; Feely et al., 2009). Associated SST cooling also increases pH (Midorikawa et al., 2010). April-May-June (AMJ) is a warm SST season in the northern IO causing the ocean to be slightly more acidic during this time which is clearly reflected in the contrast of pH values between this region and the higher alkaline STIO region during this period (Bollasina & Nigam, 2009; Dommenget, 2011; Sasamal, 2007). During JAS, the upwelling in the Arabian Sea is more intense (Emeis et al., 1995), causing the WAS to be highly acidic, with values reaching around 8.01 units. The Southern IO appears to be highly alkaline in the southwest monsoon season with cold SST where the release of H^+ ions is less common in a colder environment (Bollasina & Nigam, 2009; Midorikawa et al., 2010). Also, the presence of subtropical anticyclonic gyre, which has strong downwelling at the center decreases DIC and increases the pH (towards more alkaline) in the southern part of the IO. During OND the northwest monsoon causes pH to be slightly alkaline in the WAS (Fassbender et al., 2011). The Southern IO slowly turns acidic as the JFM approaches. The contours of OTTM pH are concurrent with the (Takahashi et al., 2014) observation of pH changes in the ocean.

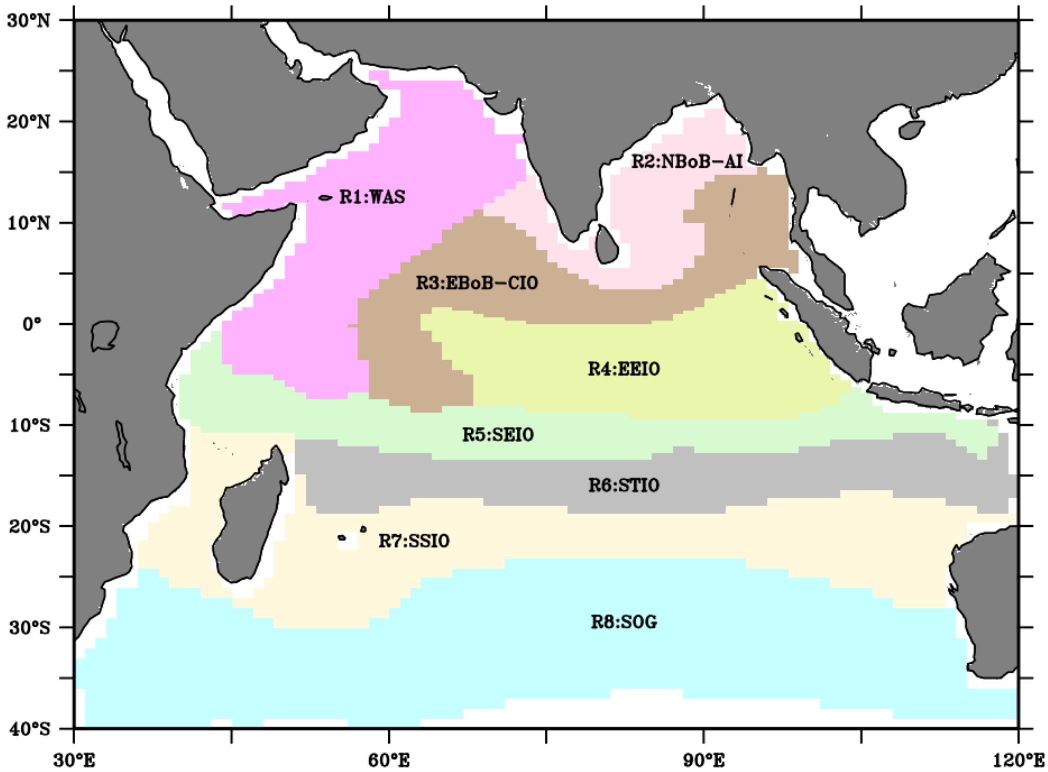

Figure S1. Different Indian Ocean bioprovinces (Source: (Sreeush et al., 2020))

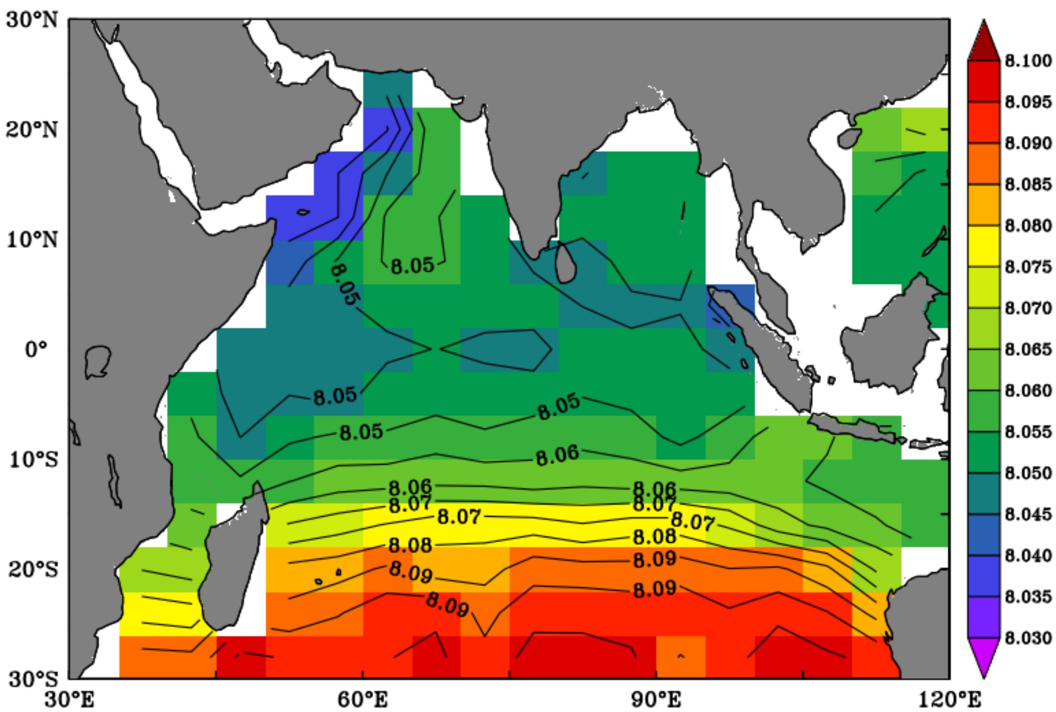

Figure S2. Annual average pH over the IO (Takahashi et al., 2014)

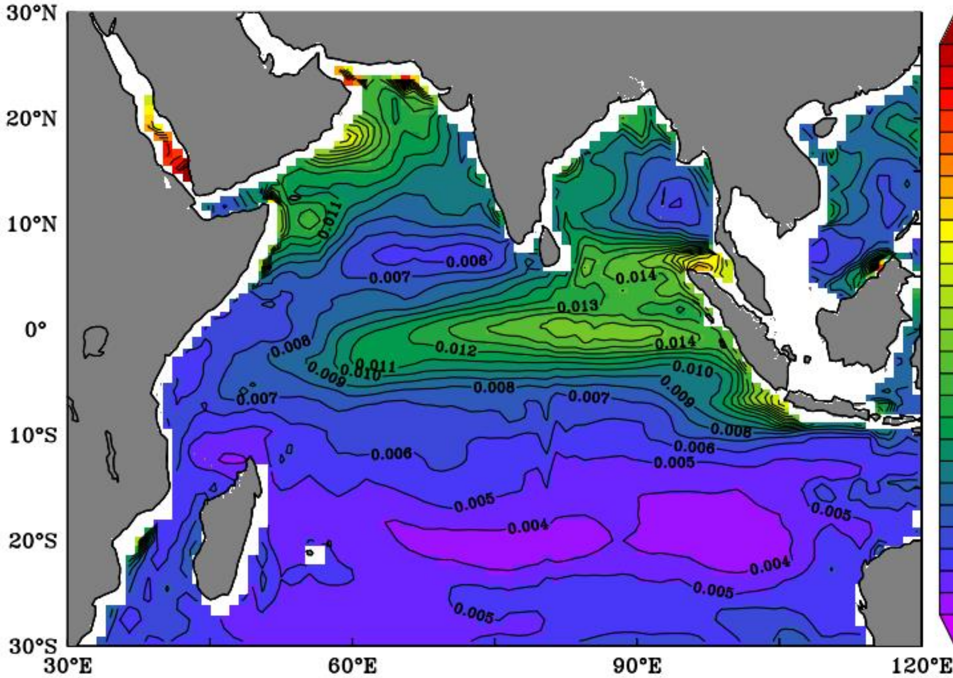

Figure S3. RMSD between model and CTRL pH over IO.

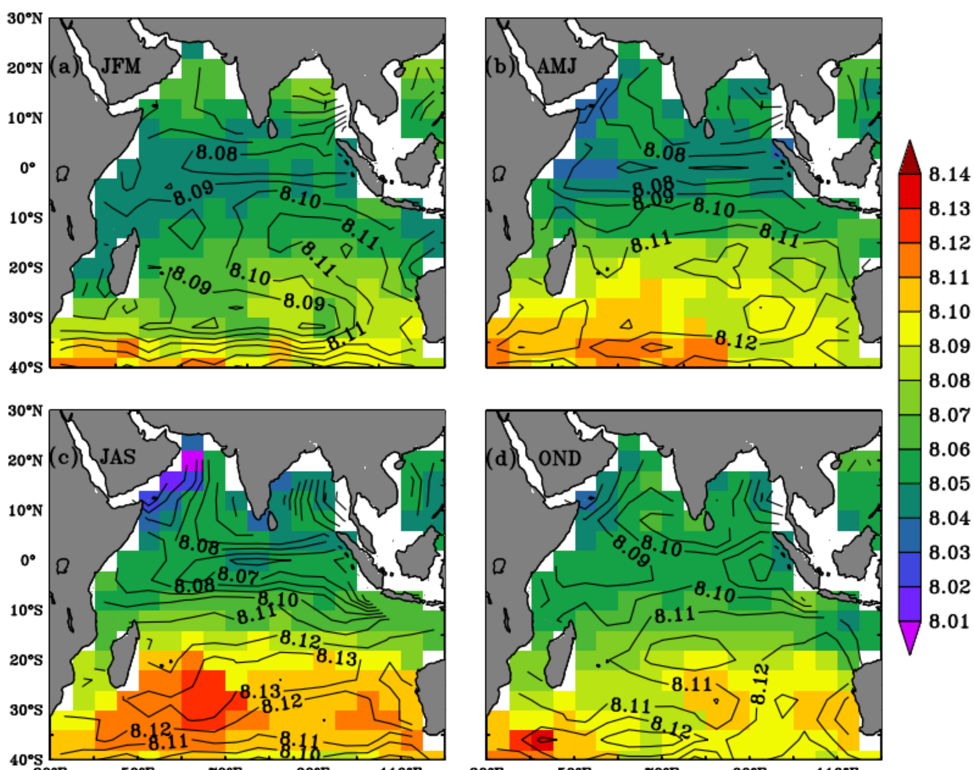

Figure S4. Seasonal mean pH over the IO (a) January to March (JFM), (b) April to June (AMJ), (c) July to September (JAS), and (d) October to December (OND). Color shades are from (Takahashi et al., 2014) and contours are from OTTM.

Table S1: Seasonal mean OTTM pH difference (ΔpH) between CTRL and Sensitivity (SENS) simulations for SST, DIC, ALK and S respectively over IO bio-provinces.

Bioprovinces	**JFM**		**AMJ**		**JAS**		**OND**	
WAS								
CTRL-SENS_SST	0.006414	±0.005	-0.02345	±0.005	0.008816	±0.002	-0.00344	±0.003
CTRL-SENS_DIC	-0.00702	±0.012	0.007785	±0.015	-0.03549	±0.003	-0.03178	±0.005
CTRL-SENS_ALK	-0.00587	±0.006	-0.00497	±0.0045	0.002269	±0.002	0.019809	±0.004
CTRL-SENS_S	-0.00146	±0.0001	-0.00111	±0.00009	-0.00068	±0.0002	-0.00092	±0.0004
NBoB-AI								
CTRL-SENS_SST	0.009288	±0.005	-0.01829	±0.003	-0.00225	±0.0008	-0.00023	±0.004
CTRL-SENS_DIC	-0.01852	±0.008	0.006533	±0.005	-0.02888	±0.002	-0.02148	±0.004
CTRL-SENS_ALK	0.007945	±0.0008	-0.00421	±0.002	0.006692	±0.0005	0.005717	±0.0006
CTRL-SENS_S	-0.00089	±0.0007	0.000142	±0.0008	-0.00167	±0.0005	-0.00067	±0.0004
EBoB-CIO								
CTRL-SENS_SST	0.000322	±0.004	-0.01453	±0.003	0.000809	±0.0009	0.001879	±0.001
CTRL-SENS_DIC	-0.02307	±0.004	-0.00182	±0.001	-0.00659	±0.001	-0.02281	±0.006
CTRL-SENS_ALK	0.004112	±0.003	-0.00681	±0.002	-0.00871	±0.004	0.022775	±0.004
CTRL-SENS_S	0.00037	±0.0008	0.000167	±0.0007	-0.00149	±0.0001	-0.00348	±0.0004
EEIO								
CTRL-SENS_SST	-0.00536	±0.002	-0.01071	±0.001	0.001874	±0.001	0.001633	±0.0005
CTRL-SENS_DIC	-0.00872	±0.002	-0.00291	±0.009	-0.05067	±0.004	-0.01325	±0.004
CTRL-SENS_ALK	0.006029	±0.001	-0.00362	±0.003	0.016177	±0.002	0.003123	±0.001
CTRL-SENS_S	0.000481	±0.0005	-0.00167	±0.001	-0.00239	±0.0004	-0.00151	±0.0001
SEIO								
CTRL-SENS_SST	-0.01851	±0.002	-0.00974	±0.007	0.018957	±0.001	-0.00242	±0.006
CTRL-SENS_DIC	0.008218	±0.002	-0.01543	±0.009	-0.03748	±0.003	-0.0101	±0.007
CTRL-SENS_ALK	-0.00965	±0.001	0.002946	±0.002	0.004588	±0.0007	0.002073	±0.002
CTRL-SENS_S	0.00121	±0.0005	0.001666	±0.0009	-0.00367	±0.0006	-0.00272	±0.0008
STIO								
CTRL-SENS_SST	-0.02159	±0.002	-0.00928	±0.007	0.019888	±0.002	0.002343	±0.007
CTRL-SENS_DIC	-0.0016	±0.002	-0.00948	±0.004	-0.02223	±0.002	-0.00545	±0.003
CTRL-SENS_ALK	-0.00079	±0.002	-0.0045	±0.002	-0.01029	±0.00006	-0.00852	±0.0008
CTRL-SENS_S	-0.00067	±0.0004	0.000637	±0.0001	-0.00088	±0.0003	-0.002	±0.0001
SSIO								
CTRL-SENS_SST	-0.02789	±0.002	-0.0091	±0.009	0.026351	±0.002	0.004576	±0.009
CTRL-SENS_DIC	0.004206	±0.001	-0.01522	±0.008	-0.03635	±0.002	-0.01564	±0.006
CTRL-SENS_ALK	-0.01042	±0.002	3.23E-05	±0.001	0.002869	±0.0003	-0.0031	±0.002
CTRL-SENS_S	0.00022	±0.0003	0.000372	±0.0003	-0.00092	±0.0001	-0.00115	±0.00006
SOG								
CTRL-SENS_SST	-0.037	±0.002	-0.00866	±0.01	0.031757	±0.003	0.004799	±0.01
CTRL-SENS_DIC	0.003427	±0.0009	-0.01866	±0.007	-0.03809	±0.002	-0.01815	±0.005
CTRL-SENS_ALK	-0.00511	±0.002	0.003376	±0.0004	0.001517	±0.0003	-0.00129	±0.002
CTRL-SENS_S	0.000104	±0.0001	0.000464	±0.0001	-5.87E-05	±0.00003	-0.00033	±0.00003

Table S2: Seasonal mean ROMS pH difference (ΔpH) between CTRL and Sensitivity (SENS) simulations for SST, DIC, ALK and S respectively over IO bio-provinces.

Bioprovinces	**JFM**		**AMJ**		**JAS**		**OND**	
WAS								
CTRL-SENS_SST	0.003786	±0.005	-0.01483	±0.006	0.011041	±0.003	5.17E-05	±0.003
CTRL-SENS_DIC	0.001037	±0.003	0.007447	±0.002	-0.00997	±0.003	0.000847	±0.001
CTRL-SENS_ALK	-0.00053	±0.00006	-0.00093	±0.00008	0.000618	±0.0005	0.000819	±0.0004
CTRL-SENS_S	0.000357	±0.0004	0.000577	±0.0003	-0.00016	±0.0001	-0.00076	±0.0001
NBoB-AI								
CTRL-SENS_SST	0.004274	±0.006	-0.01198	±0.005	0.004066	±0.001	0.00369	±0.004
CTRL-SENS_DIC	0.005065	±0.001	0.006888	±0.002	-0.00841	±0.003	-0.00389	±0.001
CTRL-SENS_ALK	-5.37E-04	±0.0001	-5.22E-04	±0.0001	0.000281	±0.0002	0.000798	±0.0002
CTRL-SENS_S	-0.00025	±0.0004	-0.00394	±0.001	0.001491	±0.002	0.003102	±0.0009
EBoB-CIO								
CTRL-SENS_SST	-0.00186	±0.004	-0.00733	±0.005	0.006427	±0.0006	0.002784	±0.0006
CTRL-SENS_DIC	0.000133	±0.0007	0.001888	±0.0003	-0.00011	±0.0008	-0.00197	±0.0002
CTRL-SENS_ALK	-0.00107	±0.0003	-0.00097	±0.00009	0.001455	±0.0006	0.000585	±0.001
CTRL-SENS_S	0.002412	±0.0002	0.000408	±0.0008	-0.00204	±0.0002	-0.00064	±0.0007
EEIO								
CTRL-SENS_SST	-0.00385	±0.002	-0.00466	±0.002	0.006628	±0.0007	0.001906	±0.001
CTRL-SENS_DIC	0.001533	±0.001	0.00313	±0.001	-0.00176	±0.0005	-0.00287	±0.0002
CTRL-SENS_ALK	-0.00164	±0.0005	-0.00178	±0.0005	0.001694	±0.0006	0.001752	±0.0004
CTRL-SENS_S	0.001433	±0.0001	-0.00017	±0.001	-0.00144	±0.0007	0.000195	±0.0002
SEIO								
CTRL-SENS_SST	-0.01501	±0.001	-0.00041	±0.006	0.018366	±0.001	-0.00288	±0.005
CTRL-SENS_DIC	0.004376	±0.001	0.001754	±0.002	-0.00386	±0.0008	-0.00159	±0.0005
CTRL-SENS_ALK	-0.00165	±0.001	-5.53E-05	±0.0008	-0.00104	±0.0003	0.002916	±0.0009
CTRL-SENS_S	0.001683	±0.0005	0.001819	±0.0008	-0.00208	±0.0002	-0.00139	±0.0001
STIO								
CTRL-SENS_SST	-0.01949	±0.001	-0.00014	±0.007	0.021284	±0.001	-0.00153	±0.006
CTRL-SENS_DIC	0.007349	±0.001	0.00379	±0.003	-0.00821	±0.0005	-0.00164	±0.002
CTRL-SENS_ALK	-0.0034	±0.0007	-0.00082	±0.001	0.003543	±0.0002	0.001174	±0.0008
CTRL-SENS_S	-3.97E-05	±0.0006	0.001526	±0.0003	-0.0001	±0.0002	-0.00137	±0.0002
SSIO								
CTRL-SENS_SST	-0.02253	±0.0008	0.000958	±0.008	0.024341	±0.001	-0.00259	±0.007
CTRL-SENS_DIC	0.003488	±0.001	0.004616	±0.001	-0.00362	±0.0009	-0.00426	±0.001
CTRL-SENS_ALK	0.001499	±0.0001	-0.00052	±0.0004	-0.00109	±0.00003	0.000266	±0.0005
CTRL-SENS_S	-9.33E-06	±0.0002	0.000445	±0.0001	0.000107	±0.00008	-0.00053	±0.0001
SOG								
CTRL-SENS_SST	-0.02878	±0.002	0.005046	±0.01	0.030764	±0.002	-0.00669	±0.01
CTRL-SENS_DIC	0.012783	±0.002	0.004795	±0.005	-0.01172	±0.0008	-0.00557	±0.003
CTRL-SENS_ALK	-0.00494	±0.0006	-0.00053	±0.002	0.00541	±0.0002	0.000932	±0.001
CTRL-SENS_S	-0.00013	±0.0002	0.000129	±0.0001	-2.8E-05	±0.00006	3.37E-05	±0.0001

Table S3: Quantification of contribution from trends in SST, DIC, ALK and S on pH trends (File uploaded separately)

Table S4: Regression coefficients in Linear trend fit for pH

Bioprovinces	JFM		AMJ		JAS		OND	
WAS								
Intercept	-0.00152	±0.00006	-0.0015	±0.0001	-0.00228	±0.00004	-0.00059	±0.00007
Slope	-0.00652	±0.0002	-0.0079	±0.0005	-0.00582	±0.0002	-0.01084	±0.0003
r2	-0.74875		-0.54202		-0.70153		-0.81995	
NBoB-AI								
Intercept	-0.00355	±0.0002	-0.00106	±0.00008	-0.00211	±0.00005	-0.00088	±0.00008
Slope	0.000999	±0.0008	-0.0123	±0.0004	-0.005	±0.0002	-0.01104	±0.0003
r2	0.07923		-0.8802		-0.85244		-0.89939	
EBoB-CIO								
Intercept	-0.00071	±0.0001	-0.0015	±0.00003	-0.00146	±0.00006	-0.00135	±0.00007
Slope	-0.00921	±0.0003	-0.00818	±0.00016	-0.0093	±0.0003	-0.0098	±0.0003
r2	-0.71098		-0.8973		-0.72677		-0.74154	
EEIO								
Intercept	-0.00158	±0.00008	-0.00169	±0.0001	-0.00186	±0.00004	-0.00207	±0.00005
Slope	-0.00754	±0.0003	-0.0075	±0.0004	-0.00689	±0.0001	-0.00685	±0.0002
r2	-0.6733		-0.52978		-0.84736		-0.72375	
SEIO								
Intercept	-0.00198	±0.00008	-0.00209	±0.0001	-0.00281	±0.00004	-0.00205	±0.0001
Slope	-0.00506	±0.0002	-0.006	±0.0005	-0.0034	±0.0002	-0.00588	±0.0004
r2	-0.66059		-0.46541		-0.55945		-0.57345	
STIO								
Intercept	-0.00188	±0.00004	-0.00064	±0.0001	-0.00236	±0.00008	-0.00124	±0.00005
Slope	-0.00438	±0.0002	-0.0105	±0.0006	-0.00215	±0.0005	-0.0078	±0.0002
r2	-0.72968		-0.62863		-0.19441		-0.81333	
SSIO								
Intercept	-0.00152	±0.00002	0.000374	±0.00006	0.000172	±0.0001	0.000238	±0.00005
Slope	-0.0075	±0.0001	-0.01719	±0.0003	-0.01423	±0.0004	-0.01535	±0.0002
r2	-0.94379		-0.91282		-0.77091		-0.9243	
SOG								
Intercept	-0.00168	±0.00004	-0.00018	±0.00005	0.000612	±0.00008	0.000207	±0.00008
Slope	-0.01188	±0.0002	-0.0156	±0.0002	-0.01397	±0.0002	-0.0149	±0.0003
r2	-0.95188		-0.96828		-0.9501		-0.93695	

Supplementary References S1

Bollasina, M., & Nigam, S. (2009). Indian Ocean SST, evaporation, and precipitation during the South Asian summer monsoon in IPCC-AR4 coupled simulations. *Climate Dynamics*, *33*(7–8). https://doi.org/10.1007/s00382-008-0477-4

Cai, W. J., Guo, X., Chen, C. T. A., Dai, M., Zhang, L., Zhai, W., et al. (2008). A comparative overview of weathering intensity and HCO3- flux in the world's major rivers with emphasis on the Changjiang, Huanghe, Zhujiang (Pearl) and Mississippi Rivers. *Continental Shelf Research*, *28*(12). https://doi.org/10.1016/j.csr.2007.10.014

Carter, B. R., Toggweiler, J. R., Key, R. M., & Sarmiento, J. L. (2014). Processes determining the marine alkalinity and calcium carbonate saturation state distributions. *Biogeosciences*, *11*(24). https://doi.org/10.5194/bg-11-7349-2014

Dommenget, D. (2011). An objective analysis of the observed spatial structure of the tropical Indian Ocean SST variability. *Climate Dynamics*, *36*(11–12). https://doi.org/10.1007/s00382-010-0787-1

Emeis, K. C., Anderson, D. M., Doose, H., Kroon, D., & Schulz-Bull, D. (1995). Sea-surface temperatures and the history of monsoon upwelling in the northwest arabian sea during the last 500,000 years. *Quaternary Research*, *43*(3). https://doi.org/10.1006/qres.1995.1041

Fassbender, A. J., Sabine, C. L., Feely, R. A., Langdon, C., & Mordy, C. W. (2011). Inorganic carbon dynamics during northern California coastal upwelling. *Continental Shelf Research*, *31*(11). https://doi.org/10.1016/j.csr.2011.04.006

Feely, R. A., Doney, S. C., & Cooley, S. R. (2009). Ocean acidification: Present conditions and future changes in a high-CO 2 world. *Oceanography*, *22*(SPL.ISS. 4). https://doi.org/10.5670/oceanog.2009.95

Land, P. E., Shutler, J. D., Findlay, H. S., Girard-Ardhuin, F., Sabia, R., Reul, N., et al. (2015). Salinity from space unlocks satellite-based assessment of ocean acidification. *Environmental Science and Technology*, *49*(4). https://doi.org/10.1021/es504849s

Midorikawa, T., Ishii, M., Saito, S., Sasano, D., Kosugi, N., Motoi, T., et al. (2010). Decreasing pH trend estimated from 25-yr time series of carbonate parameters in the western North Pacific. *Tellus, Series B: Chemical and Physical Meteorology*, *62*(5). https://doi.org/10.1111/j.1600-0889.2010.00474.x

Millero, F. J., Lee, K., & Roche, M. (1998). Distribution of alkalinity in the surface waters of the major oceans. In *Marine Chemistry* (Vol. 60). https://doi.org/10.1016/S0304-4203(97)00084-4

Sabine, C. L., Key, R. M., Feely, R. A., & Greeley, D. (2002). Inorganic carbon in the Indian Ocean: Distribution and dissolution processes. *Global Biogeochemical Cycles*, *16*(4). https://doi.org/10.1029/2002gb001869

Sabine, C. L., Feely, R. A., Gruber, N., Key, R. M., Lee, K., Bullister, J. L., et al. (2004). The oceanic sink for anthropogenic CO2. *Science*, *305*(5682). https://doi.org/10.1126/science.1097403

Sarma, V. V. S. S., Krishna, M. S., Paul, Y. S., & Murty, V. S. N. (2015). Observed changes in ocean acidity and carbon dioxide exchange in the coastal Bay of Bengal - a link to air pollution. *Tellus, Series B: Chemical and Physical Meteorology*, *67*(1). https://doi.org/10.3402/tellusb.v67.24638

Sasamal, S. K. (2007). Pre-monsoon Indian Ocean SST in contrasting years of Indian summer monsoon rainfall. *International Journal of Remote Sensing*, *28*(19). https://doi.org/10.1080/01431160500306815

Shenoi, S. S. C, D. Shankar, & Shetye, S. R. (2004). Why is Bay of Bengal warmer than Arabian Sea during the summer monsoon? *Proceedings of the National Symposium METOC*, 87–93. https://doi.org/https://drs.nio.org/drs/bitstream/handle/2264/1187/Proc_Natl_Symp_METOC_2004_87.pdf;jsessionid=DF7D0AB2B32ACE04C6E2898D5850FD2F?sequence=2

Shenoi, S. S. C., D. Shankar, & Shetye, S. R. (2002). Differences in heat budgets of the near-surface Arabian Sea and Bay of Bengal: Implications for the summer monsoon. *Journal of Geophysical Research*, *107*(C6). https://doi.org/10.1029/2000jc000679

Sompongchaiyakul, P., Chaichana, S., Bunluedaj, C., & Sukramongkol, N. (2008). Comparison of Total Phosphorus Contents and Total Alkalinity in Seawater of Different Area in the Bay of Bengal. In *The ecosystem-based fishery management in the Bay of Bengal* (pp. 17–32). Thailand. Retrieved from http://map.seafdec.org/downloads/BIMSTEC/BIMSTEC.pdf

Sreeush, M. G., Valsala, V., Santanu, H., Pentakota, S., Prasad, K. V. S. R., Naidu, C. V., & Murtugudde, R. (2020). Biological production in the Indian Ocean upwelling zones - Part 2: Data based estimates of variable compensation depth for ocean carbon models via cyclo-stationary Bayesian Inversion. *Deep-Sea Research Part II: Topical Studies in Oceanography*, *179*. https://doi.org/10.1016/j.dsr2.2019.07.007

Takahashi, T., Sutherland, S. C., Chipman, D. W., Goddard, J. G., & Ho, C. (2014). Climatological distributions of pH, pCO2, total CO2, alkalinity, and CaCO3 saturation in the global surface ocean, and temporal changes at selected locations. *Marine Chemistry*, *164*. https://doi.org/10.1016/j.marchem.2014.06.004

Trenary, L. L., & Han, W. (2008). Causes of decadal subsurface cooling in the tropical Indian Ocean during 1961-2000. *Geophysical Research Letters*, *35*(17). https://doi.org/10.1029/2008GL034687

Xie, S. P., Annamalai, H., Schott, F. A., & McCreary, J. P. (2002). Structure and mechanisms of South Indian Ocean climate variability. *Journal of Climate*, *15*(8). https://doi.org/10.1175/1520-

0442(2002)015<0864:SAMOSI>2.0.CO;2